

FIG. 5. Microstructure of magnesium near fracture surface at various temperatures, atmospheric pressure.

cavities which either linked together or reduced the actual load carrying cross-section to the point where rupture occurred.

*Low temperature.* The macroscopic fracture appearance for magnesium, as a function of pressure at  $-55^{\circ}\text{C}$ , is shown in Fig. 6. Initially, one sees a

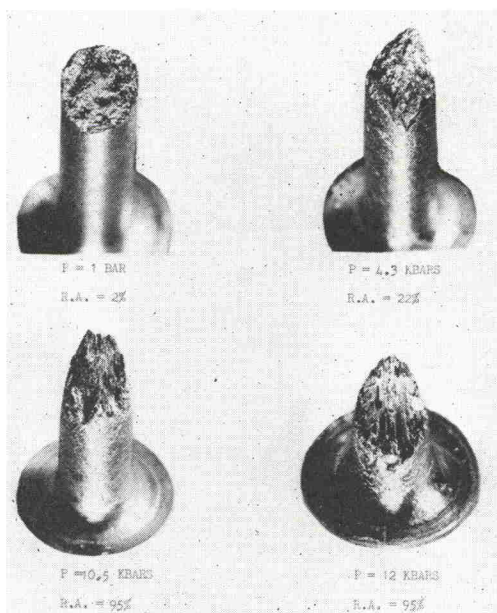


FIG. 6. Fracture appearance of magnesium as a function of pressure at  $-55^{\circ}\text{C}$ .

progressive increase in the amount of necking along with a retardation of the brittle fracture appearance and finally the onset of shear and fibrous fracture. The abrupt discontinuity in ductility shown in Fig. 3 corresponds to the fracture appearance connecting to the shear or gliding type along the shear plane as shown in the latter two photographs of Fig. 6. Above the transition pressure, no further change in fracture appearance occurred. At room temperature, the fracture appearance was much the same as at  $-55^{\circ}\text{C}$ .

Figure 7 shows a longitudinal plane through the center of a specimen above the transition pressure with the test being interrupted just prior to fracture. As can be seen, the specimen glided along the shear plane which, due to the constraint of the tensile fixture, introduced bending stresses of sufficient magnitude to severely bend the sample. The final stage of fracture involved the formation of external cracks around the periphery which penetrated inward. The crack in the center of the remaining cross-section actually was a crack initiating on the hidden surface. Since cracks do initiate at the surface at low temperatures, the gliding cannot proceed indefinitely, but still reductions in areas of 95% or greater were obtained.

The microstructural aspects of the fracture, as a function of pressure at  $-55^{\circ}\text{C}$ , are summarized in Fig. 8. At this low temperature, the initial pressure effect is to progressively retard intergranular fracture

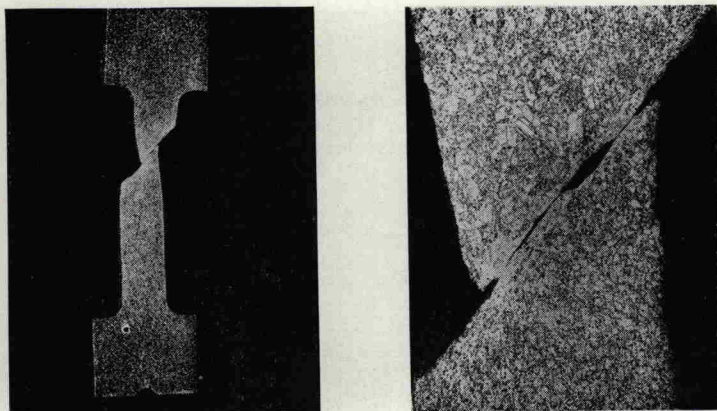


FIG. 7. Gliding type of fracturing at high pressures  $-55^{\circ}\text{C}$ .

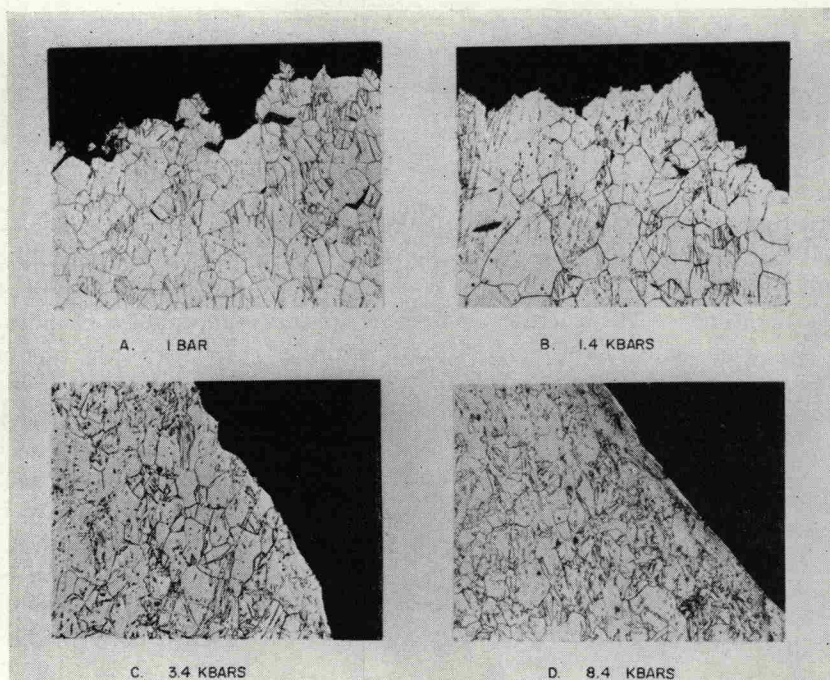


FIG. 8. Effect of pressure on fracture of magnesium at  $-55^{\circ}\text{C}$ .  $\times 150$

as shown in Figs. 8(A-C), driving the fracture mechanism towards a transgranular process similar to the fibrous type. This then corresponds to the initially linear region of the pressure-ductility curve of Fig. 3. In the region of the transition and above, the fracture is total shear along a severe localized deformation band as shown in D. When this occurs, the structure adjacent to the fracture cannot be defined.

Electron fractographs for the atmospheric pressure fracture surface shown in Fig. 8(A) and for the high pressure surface in Fig. 8(D) are shown in Figs. 9(A-B)

and (C-D) respectively. The fracture direction is towards the lower right-hand corner of each fractograph, except C, in which it is toward the lower left-hand corner. In the case of the atmospheric pressure fracture, one can see intergranular fracture A as well as dimpling B. The high-pressure fractographs (C and D) show large regions of regular ridges similar in appearance to the serpentine glide found in torsional fracture in magnesium<sup>(14)</sup> as well as large "featureless" areas. No intergranular fracture is evident. Also, there is an absence of dimples as is